



Synthesis and structural characterization of Schiff base copper(II) complexes with *Helicobacter pylori* urease inhibitory activities



Fang Niu^a, Ke-Xiang Yan^b, Linhan Pang^a, Dan Qu^a, Xinlu Zhao^a, Zhonglu You^{a,*}

^a Department of Chemistry and Chemical Engineering, Liaoning Normal University, 116029 Dalian, PR China

^b Department of Dermatology, Huashan Hospital, Shanghai 200040, PR China

ARTICLE INFO

Article history:

Received 19 May 2015

Received in revised form 28 June 2015

Accepted 7 July 2015

Available online 22 July 2015

Keywords:

Schiff base

Copper complex

Crystal structure

Urease inhibition

Molecular docking study

ABSTRACT

Three new mononuclear copper(II) complexes, [CuL¹(N₃)] (**1**), [CuL¹(NCS)] (**2**), and [CuL²(NCS)] (**3**), where L¹ is the monoanionic form of 5-diethylamino-2-[(pyridin-2-ylmethylimino)methyl]phenol (HL¹), and L² is the monoanionic form of 2-[1-(2-piperidin-1-ylethylimino)ethyl]phenol (HL²), have been synthesized and characterized by physico-chemical methods, as well as single crystal X-ray determination. The Cu atoms in the complexes are coordinated by the donor atoms of the Schiff base ligands and nitrogen atom of the pseudohalide ligands, forming square planar geometry. The complexes showed effective urease inhibitory activities. Complex **1** showed the most urease inhibitory activity, with IC₅₀ value of 1.5 ± 1.1 μM. Molecular docking study of the complexes with *Helicobacter pylori* urease was performed. As a result, complex **1** matches well with the cavity of the active center of the urease, and forms weak interaction with residues ASP316, LEU318, MET317, CYS321, HIS322 and ARG328.

© 2015 Elsevier B.V. All rights reserved.

1. Introduction

Urease is a nickel-containing metalloenzyme that catalyzes the hydrolysis of urea to form ammonia and carbamate [1,2]. The resulting carbamate spontaneously decomposes to yield ammonia and carbon dioxide. High concentration of ammonia arising from the reaction, as well as the accompanying pH elevation, has important negative implication in medicine and agriculture [3–6]. Control the activity of urease through inhibitors could counteract these negative effects [7]. Inorganic copper salts have been reported to possess potential urease inhibitory activity [8,9]. Heavy metal ions inhibit both plant and bacterial ureases at the following approximate order of effectiveness: Hg²⁺ ≈ Ag⁺ > Cu²⁺ > Ni²⁺ > Cd²⁺ > Zn²⁺ > Co²⁺ > Fe³⁺ > Pb²⁺ > Mn²⁺ [9,10]. But the application of inorganic copper salts, as well as some organic urease inhibitors, have been limited either by unsatisfied bioavailability, or by toxicity in biological system or in nature [10–12]. Consequently, it is worthy to discover and comprehensively study alternative urease inhibitors. It is proved that the cytotoxicity of inorganic metal ions can be severely decreased when they form metal complexes with organic ligands [13,14]. It can be stated that urease inhibition of transition metal complexes is influenced both by the types of ligand and metal ions. Schiff bases bearing N and O

donor atoms serve as well-known chelating agents for transition metal complexes, which show interesting biological activities [15–17]. Schiff bases also possess urease inhibitory activities [18,19]. In recent years, copper(II) complexes with a variety of Schiff bases and other medicinally attractive functionalities were intensively studied for their excellent urease inhibitory activity [20–22]. However, study on the urease inhibition of Schiff base copper complexes is still rare, and no accurate structure–activity relationship was concluded. As an extension of this work, three new copper(II) complexes, [CuL¹(N₃)] (**1**), [CuL¹(NCS)] (**2**), and [CuL²(NCS)] (**3**), where L¹ is the monoanionic form of 5-diethylamino-2-[(pyridin-2-ylmethylimino)methyl]phenol (HL¹), and L² is the monoanionic form of 2-[1-(2-piperidin-1-ylethylimino)ethyl]phenol (HL²), have been prepared and structurally characterized. Urease inhibitory activity and molecular docking analysis of the complexes with *Helicobacter pylori* urease were studied.

2. Experimental

2.1. General methods and materials

Starting material, reagents and solvents were purchased from commercial suppliers and used as received. *H. pylori* urease, HEPES (Ultra) buffer and urea (Molecular Biology Reagent) were purchased from Sigma–Aldrich. Elemental analyses were performed on a Perkin–Elmer 240C elemental analyzer. IR spectra

* Corresponding author.

E-mail address: youzhonglu@126.com (Z. You).

were recorded on a Jasco FT/IR-4000 spectrometer as KBr pellets in the 4000–400 cm^{-1} region. UV–Vis spectra were recorded on a Lambda 900 spectrometer. Molar conductance was measured with a Shanghai DDS-11A conductometer. X-ray diffraction was carried out on a Bruker SMART 1000 CCD diffractometer.

Caution: Copper perchlorate is potentially explosive, only small quantity should be used and handled with great care.

2.2. Synthesis of the complexes

[CuL¹(N₃)] (**1**): 4-Diethylaminosalicylaldehyde (0.19 g, 1.0 mmol) and 2-aminomethylpyridine (0.11 g, 1.0 mmol) were mixed and stirred in methanol (30 mL) at room temperature for 30 min. Then, sodium azide (0.065 g, 1.0 mmol) and Cu(ClO₄)₂·6H₂O (0.39 g, 1.0 mmol) dissolved in methanol (20 mL) were added to the solution. The final mixture was stirred for 30 min at room temperature to give blue solution. Upon standing at room temperature, blue block-shaped single crystals of **1** were formed. The crystals were isolated by filtration, washed three times with cold methanol and dried in air. Yield: 56%. Characteristic IR data (cm^{-1}): 2046 (s), 1595 (s), 1515 (m), 1496 (m), 1413 (w), 1387 (m), 1357 (w), 1247 (m), 1140 (m), 1071 (w), 826 (w), 758 (m), 706 (m), 661 (w), 608 (w), 570 (w), 460 (w), 416 (w). UV–Vis data in acetonitrile [λ_{max} (nm), ϵ (L mol⁻¹ cm⁻¹): 269, 20,800; 283, 18,210; 373, 17,950; 440, 18,100. *Anal. Calc.* for C₁₇H₂₀CuN₆O: C, 52.6; H, 5.2; N, 21.7. Found: C, 52.8; H, 5.3; N, 21.5%.

[CuL¹(NCS)] (**2**): Complex **2** was synthesized by the same method as that described for **1**, with sodium azide replaced by ammonium thiocyanate (0.076 g, 1.0 mmol). Blue block-shaped single crystals of **2** were obtained. Yield: 45%. Characteristic IR data (cm^{-1}): 2091 (s), 1598 (s), 1519 (m), 1496 (m), 1387 (w), 1345 (m), 1248 (m), 1138 (m), 1074 (w), 822 (w), 762 (m), 706 (w), 660 (w), 608 (w), 570 (w), 529 (w), 473 (w), 412 (w). UV–Vis data in acetonitrile [λ_{max} (nm), ϵ (L mol⁻¹ cm⁻¹): 234, 22,400; 290, 8326; 370, 28,250. *Anal. Calc.* for C₁₈H₂₀CuN₄OS: C, 53.5; H, 5.0; N, 13.9. Found: C, 53.4; H, 4.9; N, 13.8%.

[CuL²(NCS)] (**3**): 2-Acetylphenol (0.14 g, 1.0 mmol) and 2-piperidin-1-ylethylamine (0.13 g, 1.0 mmol) were mixed and stirred in methanol (30 mL) at room temperature for 30 min. Then, ammonium thiocyanate (0.076 g, 1.0 mmol) and Cu(ClO₄)₂·6H₂O (0.39 g, 1.0 mmol) dissolved in methanol (20 mL) were added to the solution. The final mixture was stirred for 30 min at room temperature to give blue solution. Upon standing at room temperature, blue block-shaped single crystals of **3** were formed. The crystals were isolated, washed three times with cold methanol and dried in air. Yield: 71%. Characteristic IR data (cm^{-1}): 2093 (s), 1600 (s), 1584 (s), 1529 (m), 1438 (m), 1352 (w), 1337 (m), 1233 (m), 1135 (w), 1037 (w), 950 (w), 862 (m), 757 (m), 635 (w), 558 (w), 527 (w), 474 (w), 448 (w), 407 (w). UV–Vis data in acetonitrile [λ_{max} (nm), ϵ (L mol⁻¹ cm⁻¹): 225, 15,600; 270, 4550; 300, 3680; 370, 2537. *Anal. Calc.* for C₁₆H₂₁CuN₃OS: C, 52.4; H, 5.8; N, 11.5. Found: C, 52.2; H, 5.8; N, 11.6%.

2.3. X-ray crystallography

Diffraction intensities for the complexes were collected at 298(2) K using a Bruker SMART 1000 CCD area-detector diffractometer with Mo K α radiation ($\lambda = 0.71073$ Å). The collected data were reduced with SAINT [23], and multi-scan absorption correction was performed using SADABS [24]. Structures of the complexes were solved by direct methods, and refined against F^2 by full-matrix least-squares methods using SHELXL [25]. All non-hydrogen atoms were refined anisotropically. Hydrogen atoms were placed in calculated positions and constrained to ride on their parent atoms. Crystallographic data for the complexes are summarized in Table 1. Selected bond lengths and angles are given in Table 2.

2.4. Urease inhibitory activity assay

H. pylori (ATCC 43,504; American Type Culture Collection, Manassas, VA) was grown in Brucella broth supplemented with 10% heat-inactivated horse serum for 24 h at 37 °C under microaerobic condition (5% O₂, 10% CO₂, and 85% N₂). For urease inhibition

Table 1
Crystallographic and experimental data for the complexes.

Complex	1	2	3
Formula	C ₁₇ H ₂₀ CuN ₆ O	C ₁₈ H ₂₀ CuN ₄ OS	C ₁₆ H ₂₁ CuN ₃ OS
<i>Mr</i>	387.9	404.0	367.0
<i>T</i> (K)	298(2)	298(2)	298(2)
Crystal shape/color	block/blue	block/blue	block/blue
Crystal size (mm ³)	0.17 × 0.15 × 0.15	0.20 × 0.20 × 0.17	0.15 × 0.13 × 0.12
Crystal system	triclinic	monoclinic	monoclinic
Space group	<i>P</i> $\bar{1}$	<i>P</i> 2 ₁ / <i>c</i>	<i>P</i> 2 ₁ / <i>n</i>
<i>a</i> (Å)	10.8608(6)	11.821(2)	11.232(6)
<i>b</i> (Å)	12.4681(7)	7.420(2)	13.139(7)
<i>c</i> (Å)	13.5926(8)	21.118(3)	11.750(6)
α (°)	79.385(1)	90	90
β (°)	74.191(1)	102.543(2)	111.31(3)
γ (°)	83.213(1)	90	90
<i>V</i> (Å ³)	1736.2(2)	1808.2(7)	1615.5(15)
<i>Z</i>	4	4	4
<i>D_c</i> (g cm ⁻³)	1.484	1.484	1.509
μ (Mo K α) (mm ⁻¹)	1.276	1.337	1.486
<i>F</i> (000)	804	836	764
Measured reflections	9164	8332	7615
Independent reflections	6390	3339	2756
Observed reflections ($I \geq 2\sigma(I)$)	5156	2550	1734
Parameters	455	228	200
Restraints	0	0	0
Min. and max. transmission	0.8123 and 0.8317	0.7759 and 0.8046	0.8079 and 0.8419
Goodness-of-fit (GOF) on F^2	1.027	1.051	0.972
R_1, wR_2 [$I \geq 2\sigma(I)$] ^a	0.0284, 0.0804	0.0357, 0.0809	0.0678, 0.1542
R_1, wR_2 (all data) ^a	0.0394, 0.0875	0.0530, 0.0888	0.1103, 0.1772

^a $R_1 = F_o - F_c/F_o$, $wR_2 = [\sum w(F_o^2 - F_c^2)]/[\sum w(F_o^2)]^{1/2}$.

Table 2
Selected bond lengths (Å) and angles (°) for the complexes.

1			
Cu1–O1	1.8972(14)	Cu1–N1	1.9309(16)
Cu1–N2	2.0107(17)	Cu1–N4	1.9527(19)
Cu2–O2	1.8943(14)	Cu2–N7	1.9362(17)
Cu2–N8	1.9957(18)	Cu2–N10	1.9631(19)
O1–Cu1–N1	94.09(7)	O1–Cu1–N4	91.55(7)
N1–Cu1–N4	173.86(8)	O1–Cu1–N2	176.10(6)
N1–Cu1–N2	82.31(7)	N4–Cu1–N2	91.99(8)
O2–Cu2–N7	93.90(7)	O2–Cu2–N10	90.42(7)
N7–Cu2–N10	175.61(8)	O2–Cu2–N8	176.35(6)
N7–Cu2–N8	82.46(7)	N10–Cu2–N8	93.22(8)
2			
Cu1–O1	1.8839(19)	Cu1–N1	1.917(2)
Cu1–N2	1.999(2)	Cu1–N4	1.939(3)
O1–Cu1–N1	93.47(9)	O1–Cu1–N4	89.55(9)
N1–Cu1–N4	176.46(10)	O1–Cu1–N2	176.06(9)
N1–Cu1–N2	82.88(10)	N4–Cu1–N2	94.15(10)
3			
Cu1–O1	1.860(5)	Cu1–N1	1.961(5)
Cu1–N2	2.054(5)	Cu1–N3	1.945(6)
O1–Cu1–N3	88.8(2)	O1–Cu1–N1	92.8(2)
N3–Cu1–N1	177.9(2)	O1–Cu1–N2	171.0(2)
N3–Cu1–N2	92.0(2)	N1–Cu1–N2	86.2(2)

assay, 50 mL broth cultures (2.0×10^8 CFU mL⁻¹) were centrifuged (5000 g, 4 °C) to collect the bacteria. After washing twice with phosphate-buffered saline (pH = 7.4), the *H. pylori* precipitation was stored at –80 °C. When *H. pylori* was returned to room temperature, and mixed with 3 mL of distilled water and protease inhibitors, sonication was performed for 60 s. Following centrifugation (15,000g, 4 °C), the supernatant was desalted through Sephadex G-25 column (PD-10 columns, Amersham-Pharmacia Biotech, Uppsala, Sweden). The resultant crude urease solution was added to an equal volume of glycerol and stored at 4 °C until use in the experiment. The assay mixture, containing 25 µL (10 U) of *H. pylori* urease which was replaced by 25 µL of cell suspension (4.0×10^7 CFU mL⁻¹) for the urease assay of intact cells and 25 µL of the test compound, was pre-incubated for 3 h at room temperature in a 96-well assay plate. Urease activity was determined by measuring ammonia production using the indophenol method as described by Weatherburn [26].

2.5. Molecular docking study

Molecular docking study of the complexes into 3D X-ray structure of *H. pylori* urease (entry 1E9Y in the Protein Data Bank) was

carried out by using AutoDock 4.0. First, AutoGrid component of the program pre-calculates a 3D grid of interaction energies based on the macromolecular target using the AMBER force field. The cubic grid box of $70 \times 70 \times 90 \text{ \AA}^3$ size (x, y, z) with a spacing of 0.375 Å and grid maps were created representing the catalytic active target site region where the native ligand was embedded. Then automated docking studies were carried out to evaluate the binding free energy of the inhibitor within the macromolecule. The GALs search algorithm (genetic algorithm with local search) was chosen to search for the best conformer. The parameters were set using the software ADT (AutoDockTools package, version 1.5.4) on PC which is associated with AutoDock 4.0. Default settings were used with an initial population of 50 randomly placed individuals, a maximum number of 2.5×10^6 energy evaluations, and a maximum number of 2.7×10^4 generations. A mutation rate of 0.02 and a crossover rate of 0.8 were chosen. Results differing by less than 0.5 Å in positional root-mean-square deviation (RMSD) were clustered together and the results of the most favorable free energy of binding were selected as the resultant complex structure.

3. Results and discussion

3.1. Chemistry

The complexes were synthesized by reaction of the Schiff bases with copper(II) chlorate and pseudohalide salts in a molar ratio of 1:1:1 in methanol. Single crystals of the complexes were obtained by slow evaporation of their methanol solutions. The complexes are stable in air at room temperature. Molar conductivity values of the complexes measured in methanol at concentration of approximately 10^{-3} M are $23.3 \Omega^{-1} \text{ cm}^2 \text{ mol}^{-1}$ for **1**, $18.7 \Omega^{-1} \text{ cm}^2 \text{ mol}^{-1}$ for **2**, and $27.7 \Omega^{-1} \text{ cm}^2 \text{ mol}^{-1}$ for **3**. The low molar conductivity values indicate non-electrolytic nature of the complexes in solution [27].

3.2. Structure description of the complexes

Single-crystal X-ray diffraction showed that the complexes are structurally similar mononuclear copper(II) species (Fig. 1 for **1**, Fig. 2 for **2**, Fig. 3 for **3**). In the asymmetric unit of **1**, there are two independent molecules. Each Cu atom in the complexes is coordinated by the NNO donor set of the Schiff base ligand, and one N atom of azide or thiocyanate ligand, forming slightly distorted square-planar geometry. The Cu atoms deviate from the least-squares planes defined by the corresponding four donor

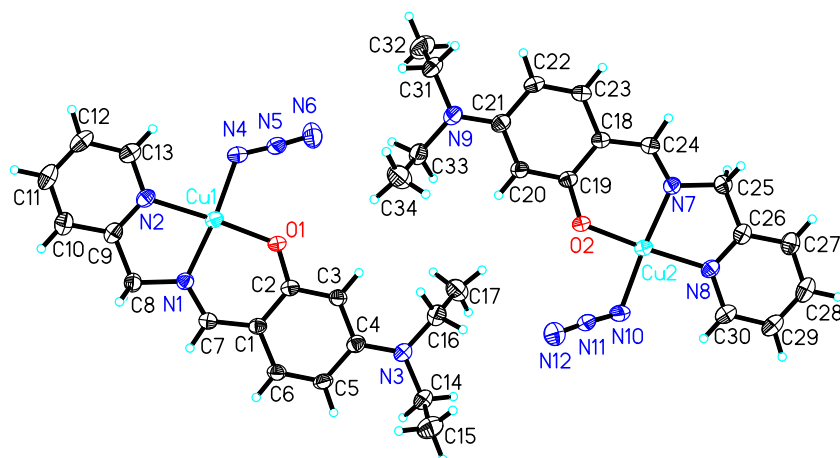


Fig. 1. A perspective view of the two independent molecules in the asymmetric unit of **1** with the atom labeling scheme. Thermal ellipsoids are drawn at the 30% probability level.

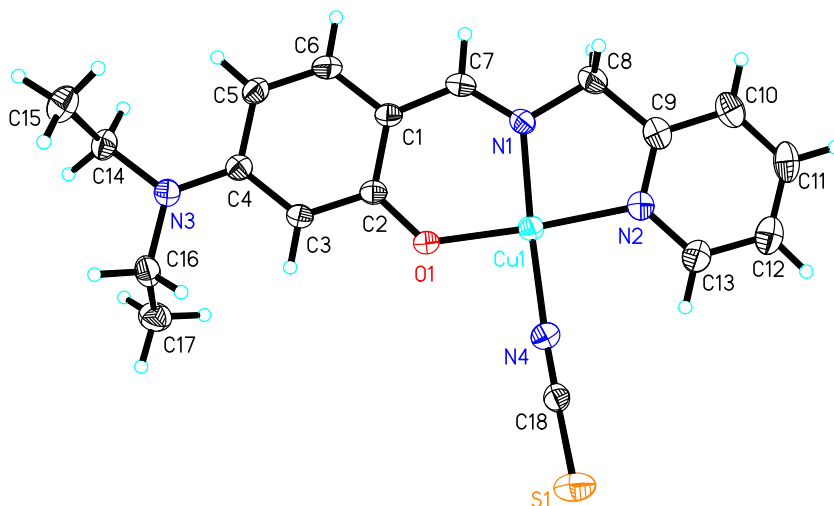


Fig. 2. A perspective view of the molecular structure of **2** with the atom labeling scheme. Thermal ellipsoids are drawn at the 30% probability level.

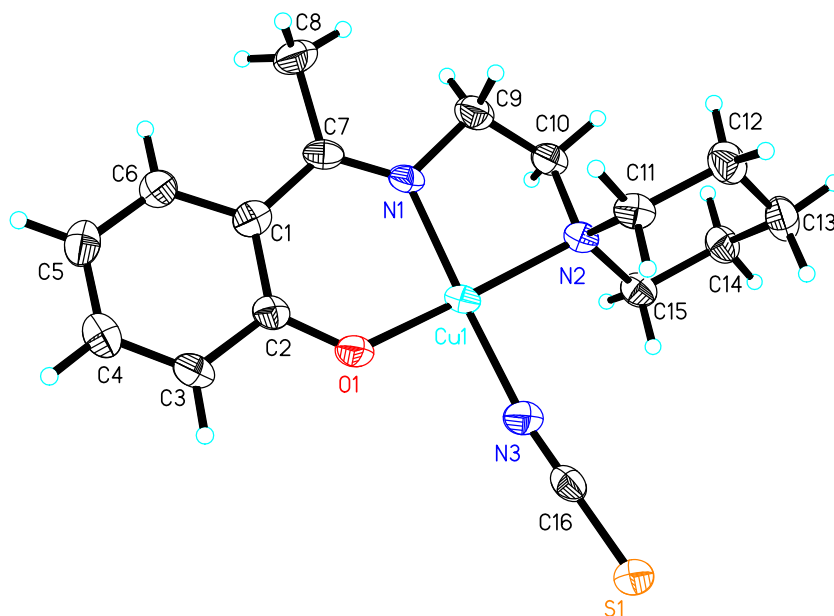


Fig. 3. A perspective view of the molecular structure of **3** with the atom labeling scheme. Thermal ellipsoids are drawn at the 30% probability level.

atoms by 0.033(2) Å for **1**, 0.004(2) Å for **2**, and 0.086(2) Å for **3**. The coordinate bond lengths related to the Cu atoms in the three complexes are similar to each other, and also comparable to those observed in copper(II) complexes with Schiff bases [28,29]. The coordinate bond angles in the complexes slightly deviate from ideal values, which is caused by the strain created by the five-membered chelate rings Cu–N–C–C–N.

The dihedral angles between benzene and pyridine rings of the Schiff base ligands are 6.9(3)° for **1**, and 3.5(3)° for **2**. As expected, the piperidine ring of **3** is in chair conformation.

3.3. IR and UV–Vis spectra

In the infrared spectrum of **1**, strong absorption band at 2046 cm^{-1} can be assigned to the vibration of the azide ligand. In the infrared spectra of **2** and **3**, strong absorption bands at about 2092 cm^{-1} can be assigned to the vibrations of the thiocyanate ligands. The typical absorption for azomethine groups, $\nu(\text{C}=\text{N})$, are observed at 1595 cm^{-1} for **1**, 1598 cm^{-1} for **2**, and 1600 cm^{-1} for

Table 3
Inhibition of urease by the tested materials.

Tested materials	Percentage Inhibition rate ^a	IC ₅₀ (μM)
1	93.0 ± 4.5	1.5 ± 1.1
2	74.1 ± 3.6	16.7 ± 3.2
3	69.2 ± 5.1	18.3 ± 2.7
HL ¹	5.5 ± 2.0	–
HL ²	3.8 ± 1.7	–
Copper perchlorate	87.5 ± 2.6	8.8 ± 1.4
Acetohydroxamic acid	84.3 ± 3.9	37.2 ± 4.0

^a The concentration of the tested material is 100 μM .

3. The medium absorption bands due to the vibration of Ar–O are located at 1247 cm^{-1} for **1**, 1248 cm^{-1} for **2**, and 1233 cm^{-1} for **3**.

The close resemblance of shape and positions of the infrared absorptions suggests similar coordination mode of the complexes, which agrees well with the structural features determined by single crystal X-ray diffraction.

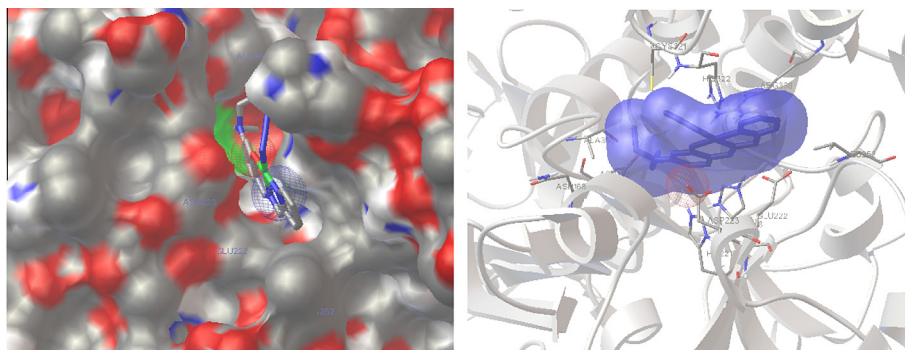


Fig. 4. Binding mode of **1** with *Helicobacter pylori* urease. Left: The enzyme is shown as surface, and the complex is shown as sticks. Hydrogen bonds are shown as wireframe. Right: The enzyme is shown as ribbons, and the complex is shown as sticks.

The electronic spectra of the complexes showed similar UV bands. The bands centered at about 370 nm originate from the phenolate to copper ion charge-transfer [30]. The intense UV bands in the range of 230–270 nm are attributed to the intra-ligand charge transfer ($\pi \rightarrow \pi^*$). However, in the electronic spectra of the complexes, the bands associated with $d \rightarrow d$ transitions are not observed, which may be due to the intensity of the charge transfer and intra-ligand transitions [31].

3.4. Pharmacology

The results of urease inhibition are summarized in Table 3. In comparison with the reference inhibitor acetohydroxamic acid, Schiff bases HL¹ and HL² have no or very weak interactions on the urease. Complexes **1**, **2**, and **3** showed effective urease inhibitory activities, with IC₅₀ values of 1.5 ± 1.1 , 16.7 ± 3.2 , and 18.3 ± 2.7 μ M, respectively, which are even lower than that of acetohydroxamic acid (IC₅₀ = 37.2 ± 4.0 μ M). Complex **1** showed prominent stronger activity than **2** and **3**. The structural difference between **1** and **2** is just the secondary ligands, viz. N₃ for **1** and NCS for **2**. As for **2** and **3**, the activities are equal within the deviations. The activity of **1** is similar to one copper complex reported by Li and co-workers, with Schiff base 2,4-dibromo-6-[[2-(4-hydroxyphenyl)ethylimino]methyl]phenol as ligand [21], and superior to the copper complexes derived from 4-nitro-2-[[2-(2-hydroxyethylamino)ethylimino]methyl]phenol [22].

3.5. Molecular docking study

Molecular docking study was performed to investigate the binding effects between the complexes and the active sites of *H. pylori* urease. In the X-ray structure available for the native *H. pylori* urease, two Ni atoms are coordinated by HIS136, HIS138, KCX219, KCX219, HIS248, HIS274, ASP362 and water molecules, while in the acetohydroxamic acid inhibited urease, the water molecules are replaced by acetohydroxamic acid. The binding model of **1** in the enzyme active site of urease is depicted in Fig. 4. The molecule of the complex matches well with the cavity of the active center of the urease, while molecules of **2** and **3** located at the outside of the cavity. The molecule of **1** forms weak interactions with residues ASP316, LEU318, MET317, CYS321, HIS322 and ARG328. The binding energy of **1** with the urease is -5.61 kcal/mol, which is lower than the acetohydroxamic acid inhibited model of -5.01 kcal/mol. The results of molecular docking study could explain the effective inhibitory activity of **1** against *H. pylori* urease.

4. Conclusion

The present study reports the synthesis, structures and urease inhibitory activity of three new mononuclear copper(II) complexes with tridentate Schiff bases. All complexes showed effective urease inhibitory activities. Complex **1** showed prominent urease inhibitory activity, with IC₅₀ value of 1.5 ± 1.1 μ M. Considering copper(II) complexes have interesting biological activities and have been widely used in medicine, complex **1** in this paper may be used in the treatment of infections caused by urease producing bacteria.

Acknowledgment

This work was financially supported by Program for Liaoning Excellent Talents in University (Project No. LR2014032).

Appendix A. Supplementary material

CCDC 940553 (**1**), 940555 (**2**), and 892372 (**3**) contains the supplementary crystallographic data for this paper. These data can be obtained free of charge from The Cambridge Crystallographic Data Centre via http://www.ccdc.cam.ac.uk/data_request/cif. Supplementary data associated with this article can be found, in the online version, at <http://dx.doi.org/10.1016/j.ica.2015.07.014>.

References

- [1] P.A. Karplus, M.A. Pearson, R.P. Hausinger, Acc. Chem. Res. 30 (1997) 330.
- [2] J.B. Sumner, J. Biol. Chem. 69 (1926) 435.
- [3] S. Bai, P. Bharti, L. Seasotiya, A. Malik, S. Dalal, Pharm. Biol. 53 (2015) 326.
- [4] D. Mora, S. Arioli, PLoS Pathog. 10 (2014) e1004472.
- [5] T.O. Brito, A.X. Souza, Y.C.C. Mota, V.S.S. Morais, L.T. de Souza, A. de Fatima, F. Macedo, L.V. Modolo, RSC Adv. 5 (2015) 44507.
- [6] K. Ni, A. Pacholski, H. Kage, Agric. Ecosyst. Environ. 197 (2014) 184.
- [7] K. Macegoniuk, A. Dzielak, A. Mucha, Ł. Berlicki, Acs Med. Chem. Lett. 6 (2015) 146.
- [8] A. Ibrar, I. Khan, N. Abbas, Arch. Pharm. Chem. Life Sci. 346 (2013) 423.
- [9] B. Krajewska, J. Mol. Catal. B Enzym. 59 (2009) 9.
- [10] W. Zaborska, B. Krajewska, Z. Olech, J. Enzyme Inhib. Med. Chem. 19 (2004) 65.
- [11] M.J. Dominguez, C. Sanmartin, M. Font, J.A. Palop, S. SanFrancisco, O. Urrutia, F. Houdusse, J. Garcia-Mina, J. Agric. Food Chem. 56 (2008) 3721.
- [12] T. von Kreybig, R. Preussmann, W. Schmidt, Arzneim. Forsch. 18 (1968) 645.
- [13] Y. Zhang, X.-D. Yang, K. Wang, D.C. Crans, J. Inorg. Biochem. 100 (2006) 80.
- [14] M.-J. Xie, X.-D. Yang, W.-P. Liu, S.-P. Yan, Z.-H. Meng, J. Inorg. Biochem. 104 (2010) 851.
- [15] L.A. Saghatforoush, F. Chalabian, A. Aminkhani, G. Karimnezhad, S. Ershad, Eur. J. Med. Chem. 44 (2009) 4490.
- [16] Z.-L. You, M. Zhang, D.-M. Xian, Dalton Trans. 41 (2012) 2515.
- [17] Z.-L. You, D.-M. Xian, M. Zhang, CrystEngComm 14 (2012) 7133.
- [18] M.A.S. Aslam, S. Mahmood, M. Shahid, A. Saeed, J. Iqbal, Eur. J. Med. Chem. 46 (2011) 5473.

- [19] A. Saeed, A. Imran, P.A. Channar, M. Shahid, W. Mahmood, J. Iqbal, *Chem. Biol. Drug Des.* 85 (2015) 225.
- [20] L. Habala, A. Roller, M. Matuska, J. Valentova, A. Rompel, F. Devinsky, *Inorg. Chim. Acta* 421 (2014) 423.
- [21] X. Dong, Y. Li, Z. Li, Y. Cui, H. Zhu, *J. Inorg. Biochem.* 108 (2012) 22.
- [22] Z.-L. You, L.-L. Ni, D.-H. Shi, S. Bai, *Eur. J. Med. Chem.* 45 (2010) 3196.
- [23] Bruker, SMART (Version 5.628) and SAINT (Version 6.02), Bruker AXS Inc., Madison, Wisconsin, USA (1998).
- [24] G.M. Sheldrick, SADABS Program for Empirical Absorption Correction of Area Detector, University of Göttingen, Germany, 1996.
- [25] G.M. Sheldrick, SHELXTL V5.1 Software Reference Manual, Bruker AXS Inc, Madison, Wisconsin, USA, 1997.
- [26] M.W. Weatherburn, *Anal. Chem.* 39 (1967) 971.
- [27] W.J. Geary, *Coord. Chem. Rev.* 7 (1971) 81.
- [28] R. Karmakar, C.R. Choudhury, D.L. Hughes, G.P.A. Yap, M.S. El Fallah, C. Desplanches, J.-P. Sutter, S. Mitra, *Inorg. Chim. Acta* 359 (2006) 1184.
- [29] C. Adhikary, D. Mal, K. Okamoto, S. Chaudhuri, S. Koner, *Polyhedron* 25 (2006) 2191.
- [30] T. Szabo-Planka, B. Gyurcsik, N.V. Nagy, A. Rockenbauer, R. Sipos, J. Sima, M. Melnik, *J. Inorg. Biochem.* 102 (2008) 101.
- [31] I. Castillo, J.M. Fernandez-Gonzalez, J.L. Garate-Morales, *J. Mol. Struct.* 657 (2003) 25.